Efficacy of Nano-Clay Derived from Egyptian Alluvial Soils for Cu(II) Removal from Aqueous Solutions

Eman M. Saleh [1], F.M. Kishk[1], Ramzy M.R. Hedia[1], Ahmed A. El-Shafei [2], Mona M. Abd El-Latif [3]

ABSTRACT

The objectives of this study were to prepare and characterize nano-clay particles from an alluvial Nile Delta Egyptian soil and to understand and evaluate its efficacy for removal of Cu(II) from aqueous solutions. Nano-clay particles were prepared by ball milling of the clay soil fraction and their nano scale was confirmed by SEM image analysis. The XRD peaks revealed the dominance of montmorillonite clay minerals in soil clay and nano-clay adsorbents. FTIR features indicated the characteristic surface functional groups of smectite clays for both adsorbents. Cu(II) adsorption by the two adsorbents tended to increase with increasing initial Cu(II) concentration (10 to 150 mg L^{-1}), adsorbent dosage (0.05, 0.1, 0.25, 0.5, 1 g/100 ml) and pH (4, 7 and 9). The two adsorbents showed high buffering capacity of the solution pH. Nano-clay adsorbent could remove higher amounts of Cu(II) from aqueous solutions (62%) than soil clay (45%) at initial Cu(II) concentration of 50 mg L^{-1} in the aqueous solution. Equilibrium time of 30 min. was achieved under the various experimental conditions which suggests ion exchange mechanism. Data of adsorption isotherms and kinetics were statistically best fitted to pseudo-second order and Langmuir models, respectively.

Keywords: Adsorption kinetics, copper ions, nano-clay, clay, adsorption.

INTRODUCTION

Reuse of wastewater can minimize the continuously increasing gap between national water resources and demands. However, cheap, and suitable techniques of wastewater treatments represent a challenge to produce massive amounts of reusable water on a national scale (Mostafa and Peters 2016). Industrial wastewater and agricultural drainage water resemble the largest sources of wastewaters. Toxic heavy metals (e.g., Cu, Zn, Cd, Cr, Ni) are the prevalent contaminants in industrial wastewater. While existing at very low concentration in wastewater, these heavy metals can accumulate in human body by direct ingestion or indirect route through the food chain (Argun et al., 2008).

Because of their accumulation in living organisms, copper metal ion (Cu^{2+}) has become a major ecotoxicological concern of growing importance (Karabulut et al. 2000). Copper is a common hazardous pollutant found in industrial wastewater, and it is frequently released to water bodies by the metallurgical, plating, electric circuits, algae treatment, industrial and mining wastes, wood preservatives, fertilizers, excessive use of Cu-based agrochemicals, and refining industries. An excessive amount of Cu^{2+} taken orally for an extended period can cause liver damage and acute poisoning in humans (WHO, 1971). Copper levels in drinking water must be less than 3 mg/L to be considered safe (Murley, 1992).

Among the recent methods that applied to remove water pollutants, adsorption technique has been an effective low cost and highly efficient approach of eliminating trace metals from wastewater and water supplies (Oei, et al., 2009). Many investigations proved the effectiveness of clays and clay minerals as sorbents for several heavy metals and their removal from wastewaters (Uddin, 2017).

Clays are hydrous aluminosilicates comprising a combination of fine-grained clay minerals, mineral crystals, and metal oxides (Mockovciakova and Orolinova, 2009). Clays and nano-clays as adsorbents have many advantages over many other commercially available adsorbents, including reasonable cost, non-toxic behaviour, high specific surface area, abundant availability, excellent adsorption characteristics, and broad ion exchange capacity (Crini and Badot, 2010). A variety of complex adsorption mechanisms; including direct bonding between metal cations and clay mineral surfaces, surface complexation, and ion exchange, contribute to the adsorption of heavy metal by clay minerals (Churchman et al., 2006). Moreover, nano sized clay particles proved to have higher surface area, exposed adsorption sites, and hence better adsorption capacities at lower dosage compared to natural clay particles (Soleimani and Siahpoosh, 2015).

Kishk et al. (1976) found that the mineral composition of the clay fraction of alluvial soils of the Nile River and Delta in Egypt contains montmorillonite

(48-56 %), kaolinite (15-18 %), mica (5-11 %), feldspars (5 %), quartz (3-5 %), and free oxides (11-16 %). Since these soils contain around 50 % montmorillonite of their clay fraction, it can be utilized as a source of efficient and safe adsorbents for removal of heavy metals from contaminated water.

Therefore, the objectives of this study were to 1) investigate the efficacy of clay and nano-clay derived from an Egyptian alluvial soil to remove copper ions from aqueous solutions, 2) understand the adsorption mechanism by analyzing the physical and chemical properties of nano-clay, and 3) evaluate Cu^{2+} ions removal kinetics and thermodynamics.

MATERIALS AND METHODS

1- Preparation of the nano-clay adsorbent:

The natural nano-clay adsorbent was obtained by separation of the clay fraction of an alluvial soil collected from Itay-Elbaroud Agricultural Research Station, El-Beheira Governorate, Egypt (30° 53´33.91´´N and 30° 38´16.81´´ E). A composite sample was obtained from five soil samples collected randomly from the top 15 cm-depth at the field, air-dried, grinded, and sieved at <2 mm. The main soil physical and chemical characteristics were determined (Table 1) according to Page and Klute (1986). A pretreatment was performed on the soil sample to remove salts, carbonates and organic matter using distilled water, sodium acetate (0.5M) and, 30% hydrogen peroxide, respectively (Kunze and Dixon, 1986). The soil was carefully rinsed with distilled water to eliminate traces of sodium acetate and hydrogen peroxide. The pretreated soil material was mechanically dispersed and disaggregated in 2-L cylinders using distilled water and then let to stand for 24 hrs for sedimentation. The fine fraction (<2 μm) was siphoned and then dried in an oven at 40°C for 72 hrs. After grinding, the collected clay particles have been passed through 250 μm sieve and stored in a plastic container for subsequent use. Synthesis of nanoscale clay particles was achieved mechanically using a ball mill (E-max Retch). The milling process was performed at 700 rpm disk speed for 3 hrs.

Table 1. Some physical and chemical characteristics of Itay-Elbaroud soil

Characteristics	value	Characteristics	value
EC, dSm^{-1}	1.23	pH	8.36
Sand, %	5	CaCO$_3$, %	4.79
Silt, %	19	OM, %	4.38
Clay, %	76	CEC, cmol$_c$ kg^{-1} soil	57
Textural class	Clay		

OM: Organic matter, CEC: Cation Exchange Capacity

2- Physicochemical characterization of nano-clay:

The characteristics and element contents of the nanoclay were investigated using a scanning electron microscopy (SEM, JEOL, Model JSM 6360 LA, Japan) coupled with energy dispersive spectroscopy (EDAX) to examine the surface morphology and elemental composition. Fourier transform infrared (FT-IR) spectroscopy analysis was carried out in the range of 400–4000 cm^{-1} using the KBr pellet technique to study the compositional properties and the functional groups of the nanoclay surface using SHEMATZU infra-red spectrophotometer (model FT/IR- 5300, JASCO Corporation, Japan). X-ray diffraction (XRD) was performed on an X-ray diffractometer (SHIMADZU - XRD-7000) with Cu-Kα radiation operated at 30 kV and 30 mA and scanning for 2θ range from 5 to 90°. Surface area of the adsorbents was determined using N$_2$ sorption isotherms run on a surface area meter (BElSORP-mini II) and the Brunauer-Emmett-Teller (BET) method (Kuila and Prasad 2013).

3- Adsorption Experiments:

To investigate the adsorption efficacy of the nano-clay for removal of Cu(II) ions from aqueous solutions, several adsorption experiments were conducted using a batch isothermal reactor. A constant temperature circulating pump (Cole Parmer Model 126-02; Cole Parmer, Illinois, USA) was used to control water flow through five 1000-mL stainless steel, double jacket-reaction vessels (Fig. 1). The reaction vessels were sealed by covers having three holes for pH electrode, thermometer, and subsample withdrawal. Subsamples of the suspensions were withdrawn by Nalgene syringe and filtered using a 0.45 μm Millipore membrane filter. All experiments were performed in triplicate. A 0.01M CaCl$_2$ as a background electrolyte and solutions were analyzed for Cu by AAS (Varian spectra AA Model 220) using air-acetylene flame. A series of stepwise experiments were carried out to study the adsorption behaviour of Cu(II) ions on clay and nano-clay as affected by pH of suspension, adsorbent dosage and initial Cu(II) concentration.

For the effect of suspension pH, the pH of adsorbent suspensions (5 g L^{-1}) was adjusted at 4, 7, and 9 using HCl or NaOH. An equal volume of Cu(NO$_3$)$_2$ with initial Cu(II) concentration (20 mg L^{-1}) was mixed, stirred at 400 rpm and subsamples were taken from the reactor time at 30, 60, and 120 min at 25 ºC. Suspensions were filtered using microfilters (0.45 μm) and the aliquots were analyzed for Cu(II).
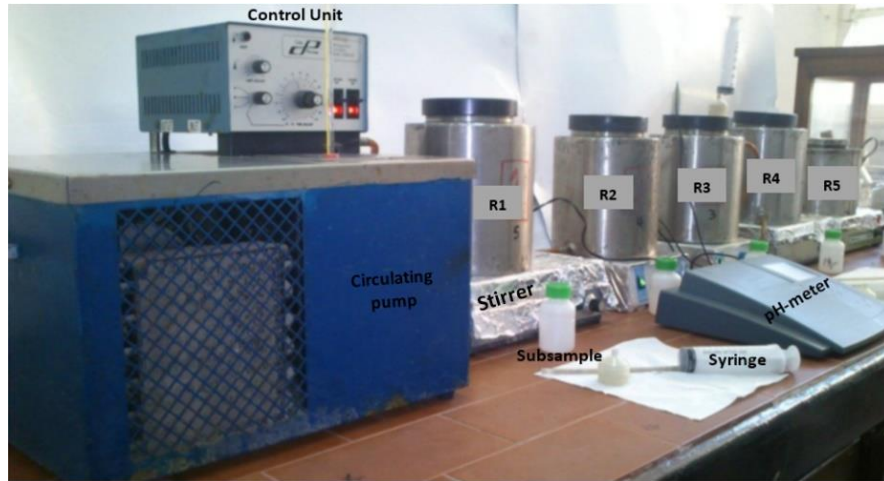
Fig. 1. Batch isothermal reactor used for adsorption experiments with five double jacket-reactor vessels (R1-5)

To find the optimal clay and nano-clay dosage, different adsorbent dosages (0.05, 0.1, 0.25, 0.5, 1 g/100 ml) were suspended in 100 ml 0.01 M CaCl$_2$ containing 20 mg L^{-1} Cu(II) and shaken for 2 hrs at 25°C.

The effect of temperature on Cu(II) removal was studied using 50 mg L^{-1} Cu(II) initial concentration at optimal sorbent dosage and pH at different temperatures (25, 35,45 and 55°C).

The amount of Cu(II) adsorbed (q$_e$, mg g^{-1} sorbent) was calculated as the amount of Cu(II) ions adsorbed in mg per gram of sorbent using the following formula (Soleimani and Siahpoosh, 2015):

$$q_e = \frac{(C_0 - C_e)}{m} \times V \quad ...... (1)$$

where q$_e$: amount adsorbate (mg g^{-1} of adsorbent), C$_0$: initial Cu(II) concentration (mg L^{-1}), C$_e$: equilibrium concentration (mg L^{-1}), m: mass of adsorbent (g), V: volume of solution (L). The percent of removal of Cu(II) ions from solution was calculated by the following equation (Soleimani and Siahpoosh, 2015):

$$Removal\ (\%) = \frac{(C_0 - C_e)}{C_0} \times 100 \quad ...... (2)$$

To investigate the effect of initial ion concentration and contact time on the adsorption of Cu(II) on clay and nano-clay, adsorption experiments were conducted in series of reaction vessels. An adsorbent dose of 2.5 gm L^{-1} was added into the reaction vessels with 1000 mL aqueous solution of different initial Cu(II) concentrations (10, 25, 50,100 and 150 mgL^{-1}) with 0.01M CaCl$_2$ solution as a background solution and at normal pH (6.8-7). Suspensions were continuously stirred at 400 rpm and at 25°C for 24 h. Sequential subsamples of suspensions (20 ml) were withdrawn

from the reaction vessel at different time intervals (5, 10, 15, 20, 30, and 45 min, 1, 1.5, 2, 12, and 24 hrs) for each initial Cu(II) concentration, filtered using 0.45μm filter membrane and analysed for Cu concentration measurement. Adsorption kinetics data (q$_t$ $vs.$ t) were fitted to four kinetics mathematical models which included:

Pseudo-first order model :

$$log(q_e - q_t) = log q_e - \frac{k_1}{2.303} t \quad ....(3)$$

Pseudo-second order model :

$$\frac{t}{q_t} = \frac{1}{k_2\,q_e^2} + \frac{1}{q_e} t \quad ....(4)$$

Intra-particle diffusion model:

$$q_t = k_{int}\,t^{\frac{1}{2}} \quad ....(5)$$

Elovich model:

$$q_t = (1/\beta)\,ln(\alpha\beta) + \left(\frac{1}{\beta}\right) ln t \quad ....(6)$$

where q_e and q_t is Cu adsorbed (mg kg^{-1}) at equilibrium and at time t,respectively ,k_1, k$_2$ and k$_{int}$ are pseudo-first order, pseudo-second order and intraparticle diffusion model rate coefficient, α is the initial adsorption rate (mg g^{-1} min^{-1}), β is a constant related to the extent of surface coverage (mg g^{-1}), t is reaction time (min) (Islam et al.,2004).

The adsorption isotherms (q$_e$ $vs.$ C$_e$) were fitted to Freundlich, Langmuir, Temkin, Dubinin- Radushkevich, Flory-Huggins, Elovich, and Hill-Debour isotherm models (Ayawei et al., 2017). In both cases, the best fit model was considered the one which had the highest

regression determination coefficient (R^2) and the lowest standard error of estimates (SE) among the tested models (Le Roux et al., 1991).

To determine the thermodynamic parameters, data of the adsorption isotherms at different temperatures was used to calculate the change in Gibbs free energy ($\Delta G°$), enthalpy ($\Delta H°$) and entropy ($\Delta S°$) as follows (Sheela et al., 2012):

$$\Delta G° = -RT\, lnk_L \qquad \ldots (7)$$

$$lnk_L = \left(\frac{\Delta S°}{R}\right) - \left(\frac{\Delta H°}{RT}\right) \qquad \ldots (8)$$

$$\Delta S° = \frac{(\Delta H° - \Delta G°)}{T} \qquad \ldots (9)$$

where R is the universal gas constant (8.314 J·mol^{-1}·K^{-1}); T is the absolute temperature (°K), and k_L is the Langmuir constant (mol·L^{-1}). $\Delta S°$ and $\Delta H°$ could be obtained from the slope and intercept lnk_L vs $1/T$ according to equation (8).

RESULTS AND DISCUSSION

1- Characterization of Nano-clay adsorbents:

1.1. Characterization of Adsorbents:

Figure (2) illustrates the image of scanning electron microscope (SEM) of the Nano-clay particles prepared by ball milling. The image shows the platy structure and the typical surface morphology of the Nano-Clay adsorbent which is a characteristic of clay minerals. The sizes of Nano-Clay granules were in the range of nano scale (less than 1 micron). The platy nano-clay particles also appear to stick together to form aggregates of different shapes and sizes. This configuration is expected to create multiple interlayer spacings.
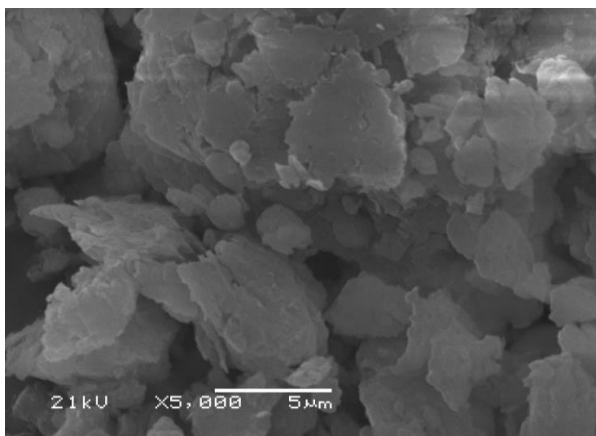

Fig. 2. SEM image of Nano-clay (N-Clay)

These results indicate that the preparation of nano-clay particles by ball milling did not affect the platy crystal structure of soil clay minerals. Similar results were obtained by Vertuccio et al. (2009) and Landry et al. (2008) who observed the stability of the structure of clay minerals during the preparation of the nanoscale particles by mechanical methods.

1.2. Energy dispersive X-ray analysis (EDAX):

Results of EDAX analysis of Clay and N-Clay adsorbents (Fig. 3) revealed that Al and Si elements are the major constituents in both the Clay and N-Clay structure. Peaks of Al and Si were observed at 1.486 and 1.739 keV, respectively (Sivasaravanan and Raja 2014). Feature peaks of Na (1.041 keV), Mg (1.253 keV), K (3. 312 keV) and Fe (6. 398 keV) were identified with mass percentages of 2.43, 4.58, 3.39, and 9.57 % respectively. These results assured the dominance of dioctahedral clay structure in the two investigated adsorbents. These results agree with those obtained by Osabor et al. (2009) and Kianfar et al. (2014).

1.3. X-Ray Diffraction Analysis (XRD):

Powder XRD diffractograms were used to elucidate the clay structures and surface properties (Mukasa-Tebandeke et al., 2015). The XRD patterns (Fig. 4) revealed the existence of montmorillonite (M) and kaolinite (K) and quartz (Q). XRD patterns of Clay and N-Clay align with those of the commercial montmorillonite (Mont.) indicating the dominance of montmorillonite clay minerals in the two adsorbents. The characteristic peaks of montmorillonite appeared at angle 2θ of 6.08°, 19.92°, 35.12°, 45.8°, 62.32° and 73.56° which relate to the interlayer spacing of the montmorillonite

(Peter, 1986; Flogeac et al 2005 ; Cintrón Alvarado et al. 2008). The presence of other peaks is due to the Kaolinite at 2θ of 25.05°, 26.54°, and 21.83°, quartz at 20.8°, 26.7°, 50.3° and 60.1° (Brown, 1984) and other clay types which belong to the smectite group such as illite (I) and other clay minerals with small portions such as micas (MI) vermiculite (V) which may present in Clay and N-Clay specimens. Since the intensity of peaks in XRD analysis is proportional to the amount of minerals, some peaks may not be clear and hard to detect in the XRD analysis.

Crystallinity percentage of Clay and N-Clay was calculated using Origin Pro. 8 software and it was 87.2% for Clay and 59.2% for N-Clay. The decrease in crystallinity for the nano particles (N-clay) may be attributed to the mechanical milling action which may have led to limited destruction of some mineral crystals (Sondi et al., 1997).
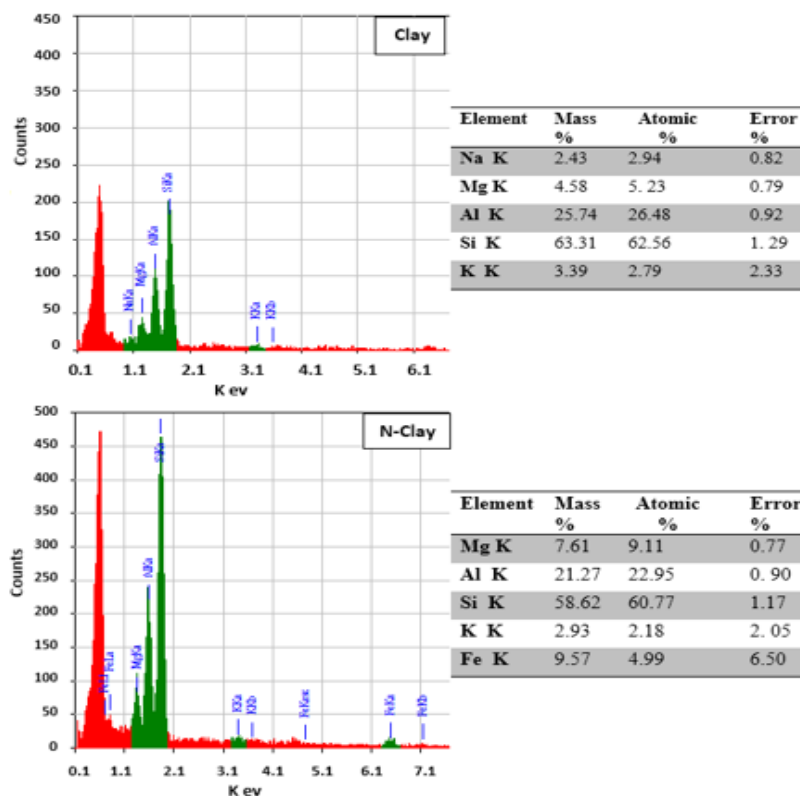
Element	Mass %	Atomic %	Error %
Na K	2.43	2.94	0.82
Mg K	4.58	5. 23	0.79
Al K	25.74	26.48	0.92
Si K	63.31	62.56	1. 29
K K	3.39	2.79	2.33

Element	Mass %	Atomic %	Error %
Mg K	7.61	9.11	0.77
Al K	21.27	22.95	0. 90
Si K	58.62	60.77	1.17
K K	2.93	2.18	2. 05
Fe K	9.57	4.99	6.50

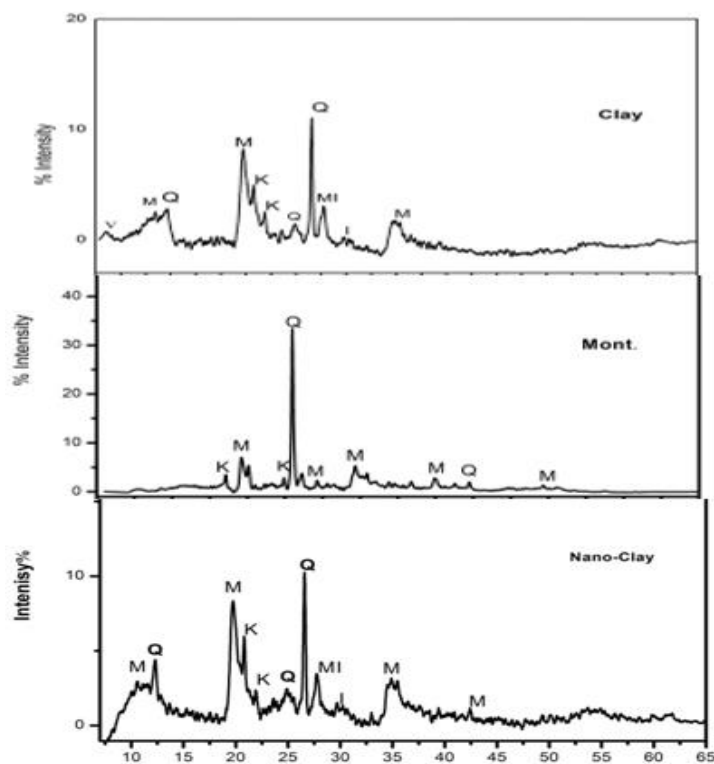**Fig. 3. EDAX analysis and elemental composition of Clay and N-Clay**

Fig. 4. XRD analysis for Clay, Mont. and Nano-Clay

1.4.Fourier Transformation Infrared Analysis (FT-IR):

IR studies on clays are very helpful to identify the behaviour of different groups which show different stretching modes at different frequencies in the infra-red region of the electromagnetic spectrum and provide specific details about the mineral structure of specimens (Madejova, 2003).

In FT-IR scan, smectites group of clay minerals show characteristic absorbance bands at 3454 cm^{-1} due to interlayer water, at 3600 cm^{-1} due to O-H, 1664 cm^{-1} due to deformational vibration in the H-O-H group, at 1042 and 798 cm^{-1} due to Si-O vibration, and the bands at 526 and 466 cm^{-1} were due to Si-O-Al and Si-O-Si deformation vibrations, respectively (Schlumberger, 1987). The IR absorption spectrum for the smectite-rich natural clays usually have absorption bands at 3640 cm^{-1} due to the presence of stretching vibrations of the OH groups while that at 3454 cm^{-1} is because of the interlayer water molecules. The portion of adsorbed water in clay layers is linked to the deformation vibrations of the H-O-H groups (1664 cm^{-1}). The bands at 1042 and 798 cm^{-1} are due to the presence of Si-O stretching vibrations (Christidis and Marcopolous, 1992). The bands at 526 and 466 cm^{-1} are attributed to deformation vibrations of Si-O-Al and Si-O-Si, respectively (Volzone et al., 1988).

The obtained FT-IR spectra (Fig. 5) showed a large similarity between Clay and N-Clay in their absorption bands which are summarized in Table 2. Bands 2, 3, 5 and 8 are the main characteristic bands for identification of montmorillonite and montmorillonite reach clays (Madejova et al. 2001). Existence of other bands reveals the impurities and/or other minerals that are present in these clays. Splitting of the first band indicates the presence of more than one type of hydroxyl bonds due to their different absorption frequencies. This in turn shows the presence of more than one clay fraction in the same sample (Madejova, 2003).
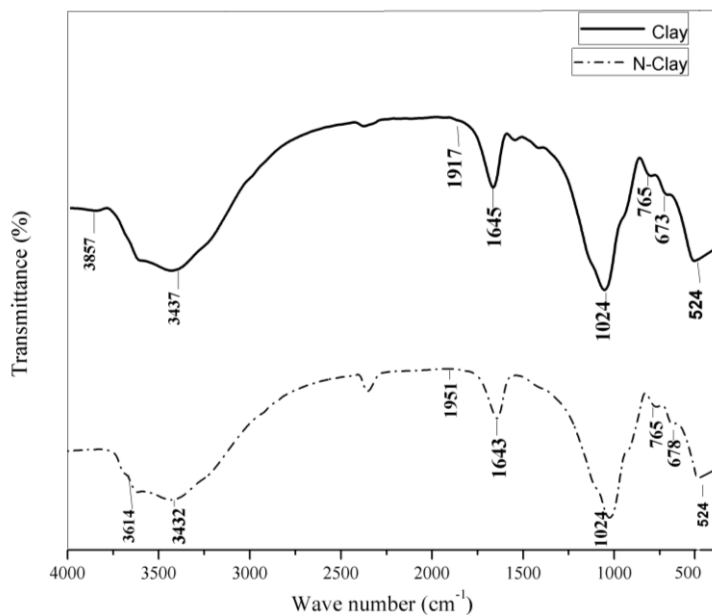

Fig. 5. FTIR spectra of Clay and N-clay

Table 2. Absorption bands in the FTIR spectra of Clay and N-Clay

Band	Functional Groups	Clay	N-Clay
1	OH stretching of structural hydroxyl groups	NA	3614
2	OH stretching of water (Interlayer water)	3437	3432
3	H-O-H	1917	1951
4	OH deformation of water	1645	1639
5	Si–O stretching	1024	1025
6	Si–O stretching of quartz and silica	765	765
7	Coupled Al–O and Si–O, out-of-plane	673	678
8	Al–O–Si deformation	524	525

1.5. Specific surface area and pore size:

Results of the specific surface area, total pore volume and mean pore diameter of Clay and N-Clay are listed in Table 3. The surface area of N-Clay was higher than that of Clay (1.11×10^2 and 9.01 m^2 g^{-1}, respectively). Comparable results for nano clays were reported by Chotpantarat and Kiatvarangkul (2018). Similarly, total pore volume of N-Clay was higher than that of Clay (10.9×10^{-2} and 9.24×10^{-2} cm^3 g^{-1}, respectively). The mean pore diameter showed an opposite trend of the surface area (Clay > N-Clay). These results agreed with those trends observed by Sondi et al. (1997) and Vdović et al. (2010).

Table 3.Specific surface area, total pore volume and mean pore diameter of Clay and N-clay

| Characteristic	Clay	N-clay
Surface area, m²/g	9.01	1.11×10^2
Total pore volume, cm³/g	9.24×10^{-2}	10.9×10^{-2}
Mean pore diameter, nm	4.10	3.94

2- Effects of different factors on Cu(II) adsorption:
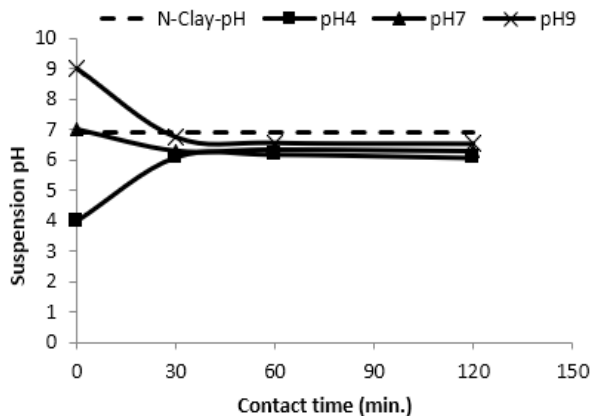
2.1. Effect of pH:

The effect of three different pH values (4, 7 and 9) of Clay, and N-Clay suspensions on Cu ions removal are shown in Figure 6. It is clear that adsorption of Cu ions increased with increasing pH of Clay and N-Clay suspensions from 4 to 9. This increase occurred likely because Cu ions were strongly bound to the hydroxyl groups on the edges of the clay minerals at higher pH value (Angove et al., 1998). However, at lower pH value, there was an excess of H_3O^+ ions which promoted competition between the positively charged

hydrogen ions and metal cations for the available adsorption sites on the negatively charged clay surface. According to Gu et al. (2010) at lower pH, the cationic metals are commonly bound to clay surfaces by forming outer-sphere surface complexes with the permanently negatively charged basal surface sites ($\equiv X-$), while at higher pH, the adsorption arises mainly on the variable charged edge sites ($\equiv SOH$) by forming an inner-sphere surface complexes. Eren and Afsin (2008) reported that adsorption of Cu(II) by bentonite is a complex procedure controlled by several environmental variables (pH, ionic strength, and the presence of Cl^-, SO_4^{2-}, PO_4^{3-}). They proposed that Cu^{+2} sorption onto bentonite occurs in two stages: The first stage includes adsorption on permanent negatively charged sites and the second

includes adsorption on variably charged sites. Similarly, Soleimani et al. (2015) and Chotpantarat and Kiatvarangkul (2018) found positive effect of increasing the pH value on Cu(II) and Cd(II) ions removal from aqueous solutions. In addition, Clay and N-Clay suspensions showed high resistance to pH changes (Fig. 7). The pH of suspensions after 30 min, from the start of the experiment, decreased by about one to two units from pH 9 to 6.5 – 7. This can be attributed to the high buffering capacity of montmorillonite, which is a characteristic of the used clay (Ouhadi et al., 2012). Yong et al. (1990) explained that clay can act as an acid or base, and thus show a resistance to pH changes specially smectites that showed a considerable resistance to pH change because of its high CEC. Chotpantarat and Kiatvarangkul (2018) suggested that adsorption of Cu(II) onto clay and its nano sized particles occurred mainly on the edge sites through the inner-sphere complex.
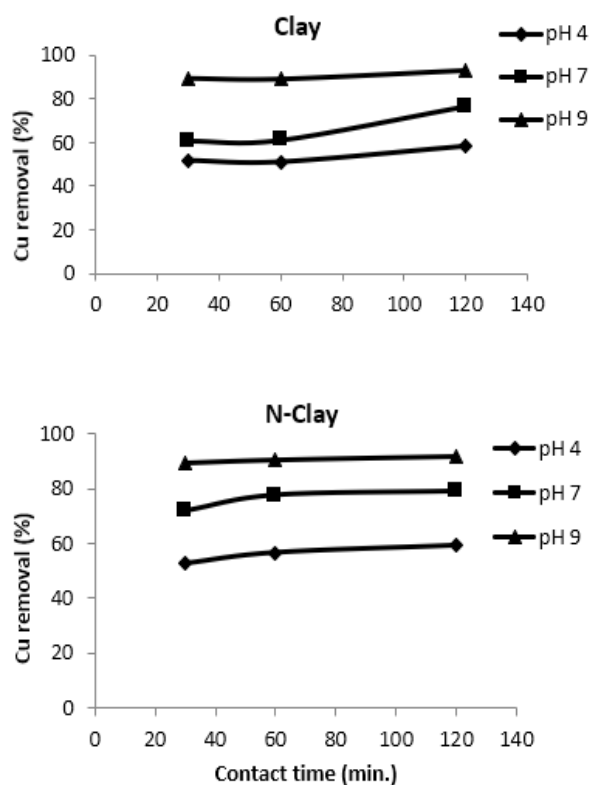
Fig. 6. Effects of contact time and suspension pH on removal of Cu ions by Clay and N-Clay

**Fig.7. Changes of pH values in N-Clay suspension with time**
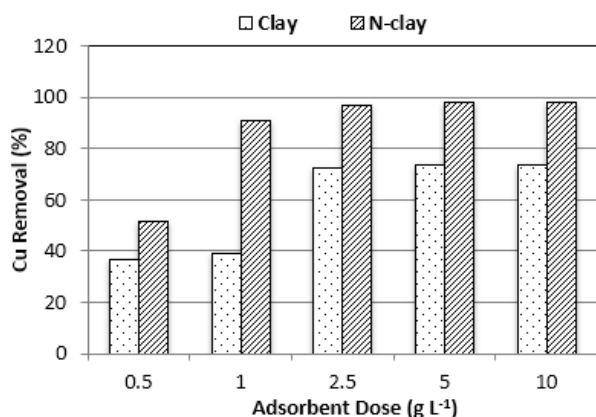
Fig. 8.Effect of adsorbent dosage on Cu(II) removal by Clay and N-clay

2.2. Effect of adsorbent dosage:

The removal of Cu(II) ions from the aqueous solutions increased as the doses of the Clay, and Nano-clay were increased from 0.5 to 10.0 g L^{-1} (Fig. 8). However, the Cu(II) ions removal percentage did not show a significant increase at adsorbent doses higher than 2.5 g L^{-1}. This may be due to higher probability of collision and more chances for metal ions to contact with the adsorption sites when the adsorbent dosage was less than 2.5 g L^{-1}. Further Increase of sorbent dosage facilitates flocculation and aggregation of Clay and N-Clay particles (Soleimani and Siahpoosh, 2016). Similar results were reported for adsorption of Pb^{+2} on sawdust (Yu et al., 2001), Cu^{+2} on palygorskite (Chen et al., 2007) and Cd^{+2} on riverbed sediments (Jain et al., 2002). Thus, it is clear from Fig. 8 that N-Clay had higher capacity to remove Cu(II) from the aqueous solution than Clay at all suspension dosages tested.

2.3. Effect of initial Cu(II) concentration:

Increasing the initial Cu(II) concentration (10, 25, 50,100 and 150 mg L^{-1}) led to an increase in the amount of Cu(II) adsorbed (q$_e$, mg Cu g^{-1} adsorbent) by both absorbents after 30 min. contact time (Fig. 9). The slope of the q$_e$ - C$_0$ curve was steep upwards till the initial Cu(II) concentration of 50 ppm indicating a high adsorption capacity of the two adsorbents. However, further increase of initial Cu(II) concentration resulted in a less slope indicating a decline in the adsorption capacity of the two adsorbents. The higher the initial concentration, the higher the removal of Cu(II) by N-Clay compared with Clay indicating higher adsorption capacity (Rezvani, and Taghizadeh. 2018)
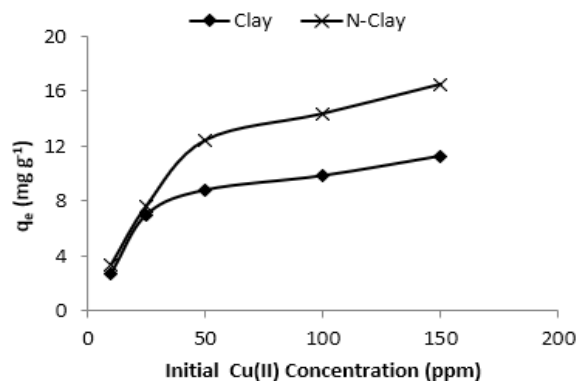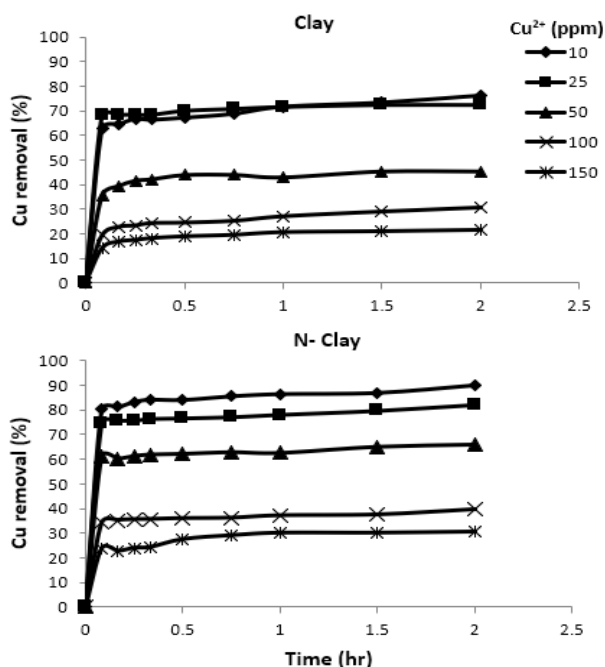

Fig. 9.The relation between initial concentration of Cu(II) in the aqueous solution and Cu(II) adsorption by Clay and N-Clay for 30 min contact time at 25 °C

These results may indicate the limited number of available adsorption sites on the surfaces of the two adsorbents at high Cu(II) concentrations. Al-Anber and Al-Anber (2008) proposed that this behavior can be related to the competitive diffusion process of the metal ions through the micro channel and pores. Such competitive behavior will lock the inlet of channel on the surface and prevents the metal ions to pass deeply inside the adsorbent material, *i.e.* the adsorption occurs on the surface only.

2.4. Effect of contact time:

To gain insight into a sorption process, the necessary contact time for adsorption to be completed is critical. This also reveals the shortest time for significant adsorption to occur, as well as the potential diffusion regulation mechanism between the adsorbent and the adsorbate (Soleimani et al., 2015).

Fig. 10. The relation between contact time and the initial Cu(II) concentration on the removal of Cu(II) by Clay and N-Clay at 25°C

Data of the effect of contact time (5, 10, 15, 20, 30, 45 min., 1, 1.5 and 2 hrs) on adsorption of Cu(II) onto the Clay and N-clay using different initial Cu(II) concentrations are shown in Fig. 10. Based on the statistical analysis of data, removal of Cu(II) increased significantly with contact time up to 30 min. For contact time greater than 30 min., no significant increase in Cu(II) removal were recorded.

The 30 min. contact time needed to reach maximum adsorption or equilibrium of the system may indicate the rapid nature of Cu(II) adsorption on the two adsorbents. Several studies on adsorption of divalent metal cations on smectites such as Cu (Soleimani et al., 2015) , Cd (Dal Bosco et al., 2006), Pb and Zn (Sipos et al., 2018) revealed that the adsorption of these metal cations is a rapid process, and their equilibrium times were of the magnitude of minutes.

2.5- Effect of temperature:

As shown in Fig.11, the higher the temperature, the lower the removal of Cu(II) from the aqueous medium by either Clay or by N-Clay. This effect may be due to increasing the kinetic energy of metal ions, increasing the activities of mineral's surface, and decreasing the resistance to mass transfer (Soleimani et al., 2015). Malamis and Kaston (2013) suggested also that higher temperature may cause a delay of basic interactions or electrostatic interactions and a physical damage to the mineral surfaces can occur at high temperatures and reduce the potential for adsorption.

Although the adsorbing potential of Cu(II) by N-Clay was higher than by Clay at 300 °K, the difference between them diminished as the temperature increased. For an effective cost of the process, the adsorbing potential of minerals must be assessed at room temperature (Malamis and Kaston 2013).
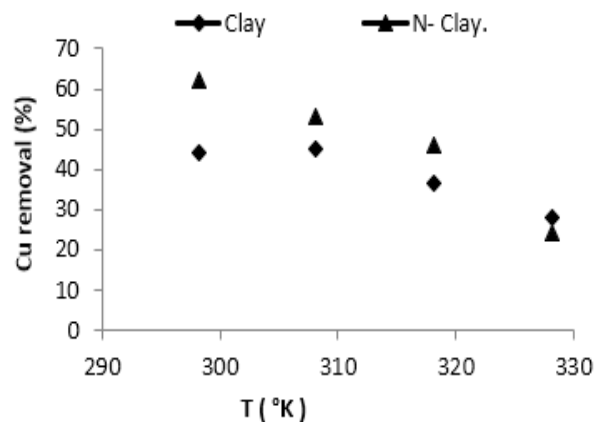
Fig. 11.Effect of temperature on the removal percentage of Cu(II) ions by Clay and N-Clay from aqueous solution (50 mg L^{-1})

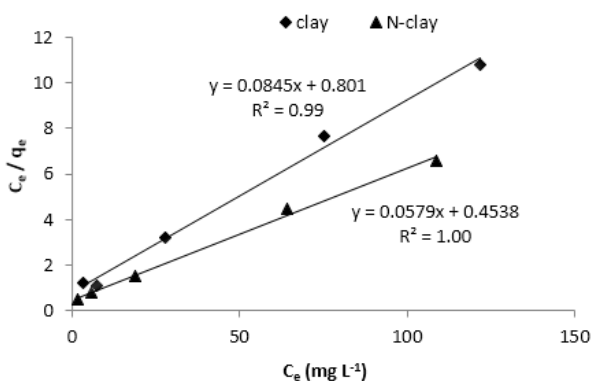### 3- Adsorption isotherms:

Fitting parameters of different isotherm mathematical models to the experimental data of Cu(II) adsorption by Clay and N-Clay are listed in Table 3. The regression determination coefficients (R^2) were moderate to high for the models tested. However, the standard errors of estimates (SE) values for Temkin, Flory-Huggins, Elovich and Hill-de Boer were high which indicates a weak predictive validity for the description of the adsorption data for these models. Langmuir and Freundlich models had the highest R^2 and the lowest SE values for both adsorbents. Because of its wider application, Langmuir isotherm model was considered the best fit to the experimental data (R^2:0.99-1.00; SE: 0.2-0.4).

The Langmuir constant K_L (L mg^{-1}) indicates the strength and affinity of the adsorbents for the solute and it can be used as an indicator for the isotherm progress in the range of low metal ion concentration (Bhattacharyya and Gupta 2005). Nano-Clay had higher K_L (1.27 L mg^{-1}) than Clay (0.1 L mg^{-1}) which indicates a higher affinity of Cu(II) towards its surface. In addition, adsorption capacity of copper (q_{max}) estimated by Langmuir model was concur with the experimental values (11.28 and 16.51 μg g^{-1} for Clay and N-Clay, respectively).

Table 3.Fitted model parameters of different adsorption isotherms for Cu(II) adsorption by Clay and N-Clay

Models	Parameters	Clay	N-Clay
Langmuir $C_e/q_e = 1/q_m K_L + C_e/q_m$	$q_{max}(\mu g\ g^{-1})$	11.83	17.27
	K_L (Lmg^{-1})	0.10	1.27
	R^2	0.99	1.00
	SE	0.40	0.20
Freundlich $\log q_e = \log K_F + 1/n \log C_e$	$K_F(mLg^{-1})$	2.49	3.45
	$1/n$	0.33	0.35
	R^2	0.80	0.92
	SE	0.13	0.09
Temkin $q_e = RT/b \ln K_T + RT/b \ln C_e$	$b(kJmol^{-1})$	11.93	8.12
	K_T (L g^{-1})	1.97	2.13
	R^2	0.91	0.98
	SE	1.14	0.79
Dubinin- Radushkevich $\ln q_e = K_{DR}\ \epsilon^2 + \ln q_{max}$	$q_{max}(\mu g\ g^{-1})$	195.02	359.91
	K_{DR}	-0.030	-0.009
	R^2	0.98	0.87
	SE	0.09	0.27
	E	4.07	7.29
Flory-Huggins $\ln(\theta/C_o) = \ln K_{FH} + n\ln(1-\theta)$	n_{FH}	-3.41	-2.38
	K_{FH}	$8.85*10^8$	$1.39*10^7$
	R^2	0.91	0.99
	SE	0.56	0.19
Elovich $\ln q_e/C_e = \ln K_e q_m - q_e/q_m$	$q_{max}(\mu g\ g^{-1})$	-3.71	-4.91
	K_E	0.55	0.46
	R^2	0.73	0.93
	SE	0.63	0.35
Hill-Debour $\ln C_e [(1-\theta)/\theta] - \theta/(1-\theta) = -\ln K_1 - K_2\theta/RT$	K_1	$7.6*10^8$	$1.33*10^{11}$
	K_2	-366.64	-472.36
	R^2	0.99	0.94
	SE	0.43	0.65

Note: q_e (mg g^{-1}) is Cu adsorbed per gram of adsorbent, C_e (mg L^{-1}) is equilibrium Cu concentration, q_{max} (mg g^{-1}) is the maximum adsorption capacity of the adsorbent, K_L (Lmg^{-1}) is Langmuir constant related to the free energy of adsorption, K_F is a constant related to adsorption capacity of the adsorbent (Lmg^{-1}), n is a constant, R is the universal gas constant (kJ mol^{-1} K^{-1}), T is the temperature (K), b is the Temkin constant related to heat of sorption (J/mole), $k_{DR} \cdot$(mol$^{-2} \cdot$J^{-2}) is a constant related to the adsorption energy, and ϵ is the maximum adsorption capacity, θ is degree of surface coverage, n is number of adsorbate settled on adsorption sites, and K_{FH} is Flory-Huggins constant (Lmol^{-1}), K_1 is Hill-de Boer constant (Lmg^{-1}), and K_2 (kJmol^{-1}) is a constant related to the interaction between adsorbed molecules. A positive K_2 means attraction between adsorbed species and a negative value means repulsion.

The larger surface area of Clay and of course N-Clay provides available surfaces for the ions to be adsorbed on a monolayer arrangement. Such kind of binding on clay surfaces explains the possibility of the adsorption isotherm to follow Langmuir isotherm. These results agreed with those obtained by Pimneva1 (2017), Yavuz et al. (2003) and Soleimani et al. (2015) who reported that adsorption isotherms of Cu^{2+} by natural nano-clays from aqueous solutions, natural water, and food samples were best fitted to Langmuir equation.

Fig.12. Langmuir isotherm for adsorption of Cu^{+2} on Clay and N-clay

A dimensionless equilibrium parameter (R_L) was calculated from Langmuir constants (K_L) obtained using the equation (Bergaya and Vayer, 1997):

$$R_{L=} \frac{1}{(1 + K_L * C_0)} \quad \dots (10)$$

where, K_L is the Langmuir constant and C_0 is the highest initial concentration applied in the experimental isotherm (150 ppm). The R_L value indicates the adsorption to be unfavorable ($R_L > 1$), linear ($R_L = 1$), favorable ($R_L < 1$), reversible ($0 < R_L < 1$) or irreversible ($R_L = 0$). Calculated R_L values were 0.06 and 0.01 for Clay and N-Clay, respectively. This indicates a favorable adsorption behavior for Cu(II) ions on the two adsorbents (Dal Bosco et al., 2006).

4- Adsorption kinetics:

The kinetics data of Cu(II) adsorption on Clay and N-Clay at different initial concentrations were fitted to four kinetic mathematical models using regression analysis and model parameters. The values of R^2 and SE are listed in Table 4.

The pseudo-second order model was the best model for both the two adsorbents, with the highest R^2 and the lowest SE values among other models (Fig. 13). The values of maximum adsorption of Cu(II) estimated from the pseudo second-order model of the Clay and Nano-Clay matched the experimental maximum adsorption capacities.
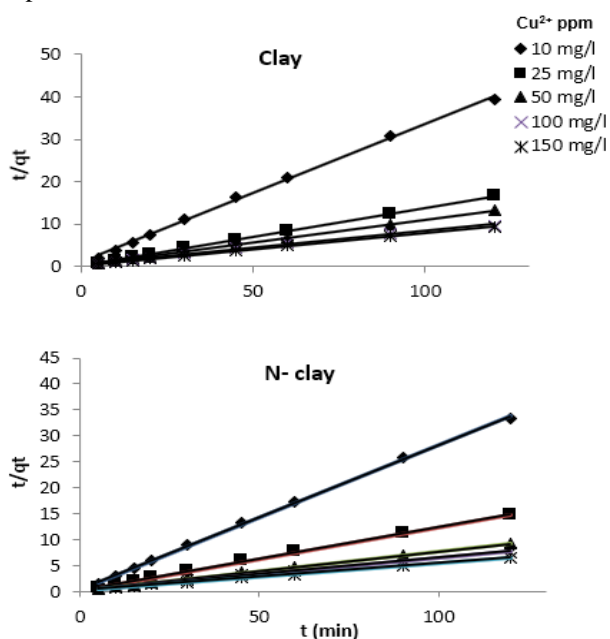

Fig. 13. Fitted pseudo-second order model of Cu(II) adsorption on Clay and N-Clay for adsorption kinetics at 25 °C

Similar kinetic studies of metal ions on various adsorbents were reported by Bhattacharyya and Gupta (2008) and Wang et al. (2007) where the Clay–Cu(II) interactions found to follow the second order mechanism. Wang et al. (2007) proposed second order kinetics for adsorption of Cu ions with the rate coefficient varying from 0.238 to 0.399 g·mg^{-1}·min^{-1} at temperatures ranged from 293 to 313 °K. Chen et al. (2007) reported also that adsorption of Cu(II) on palygorskite followed pseudo-second-order kinetic model with a relatively small contribution of film diffusion.

5- Thermodynamics parameters:

The thermodynamic constants, Gibbs free energy change (ΔG∘), enthalpy change (ΔH∘) and entropy change (ΔS∘) were calculated to evaluate the thermodynamic nature and the spontaneous nature of the adsorption process.

Gibbs Free Energy change (ΔG°): The negative values of ΔG° obtained for the adsorption of Cu(II) ions indicate that the process is thermodynamically feasible, spontaneous, and corresponding to an electrostatic adsorption process on Clay and Nano-Clay surfaces (Table 5). These negative values can provide a measure for the heavy metals binding on the clay surfaces. The stronger the metal binding, the more its negative value of ΔG°. This behavior can be correlated with the electrical, physical, and chemical properties of the two surfaces, i.e. Clay and N-Clay.

Enthalpy change (ΔH°): The enthalpy of the adsorption (ΔH°) is a measure of the energy barrier that must be overcome by reacting molecules (Ucun et al., 2008). The positive ΔH° of Cu(II) adsorption on Clay and N-Clay (Table 5) indicate an endothermic reaction of the adsorption process. Similar findings were found by Bhattacharyya and Gupta (2011; 2008). Values of ΔH° less than 20 kJ.mol^{-1} suggest that physical sorption predominate in the adsorption process. The estimated values of ΔH° for the current system were greater than 20 kJ.mol^{-1}, implying that the process may involve a spontaneous sorption mechanism such as ion exchange where chemical bonds are weak (Sheela et al., 2012).

Entropy change (ΔS°): The value of ΔS° can be used to identify whether the adsorption reaction is attributed to associative or dissociative mechanism (Ucun et al., 2008). The negative value of ΔS° obtained for Cu(II) adsorption on Nano-Clay surfaces may indicate a stable configuration of the metal ion on the surface. In contrast, the positive value ΔS^0 for Clay suggests some structural changes in the adsorbent and adsorbate configuration after the adsorption reaction (Manohar et al., 2002; Adebowale et al., 2008).

Table 4. Fitted model parameters of Cu (II) adsorption kinetics for Clay and N-Clay

C_0 mg/L	q_e mg/g	Pseudo-first order model			Pseudo-second order model			
		K_1	R^2	SE	q_e^2	K_2	R^2	SE
				Clay				
10	0.37	-6.95×10^{-4}	0.89	0.25	9.67	0.07	1.00	0.88
25	0.36	$-4.78*10^{-4}$	0.87	0.21	54.30	0.08	1.00	0.27
50	1.05	$-5.64*10^{-4}$	0.88	0.21	89.50	0.03	0.99	0.55
100	3.80	$-1.65*10^{-3}$	0.92	0.31	163.10	0.01	1.00	0.25
150	2.49	$-6.95*10^{-4}$	0.89	0.24	182.12	0.01	0.99	0.48
				Nano-Clay				
10	0.31	$-6.51*10^{-4}$	0.90	0.24	13.71	0.09	1.00	0.40
25	0.64	$-3.04*10^{-4}$	0.69	0.20	70.49	0.04	1.00	0.36
50	1.24	$-5.64*10^{-4}$	0.96	0.13	59.17	0.07	1.00	0.23
100	1.41	$-6.95*10^{-4}$	0.87	0.29	255.18	0.02	1.00	0.12
150	2.83	$-4.34*10^{-4}$	0.73	0.27	369.82	0.01	0.99	0.47

	Elovich				Intraparticle diffusion		
	α	β	R^2	SE	K_{int}	R^2	SE
			Clay				
10	8.74×10^7	8.71	0.89	0.07	0.02	0.66	0.13
25	$3.13*10^{24}$	8.85	0.87	0.08	0.02	0.63	0.13
50	$4.83*10^8$	2.91	0.77	0.33	0.02	0.49	0.51
100	$2.83*10^3$	1.14	0.89	0.55	0.11	0.62	1.03
150	$1.96*10^4$	1.22	0.85	0.63	0.10	0.53	1.10
			Nano-Clay				
10	$3.14*10^{13}$	10.88	0.95	0.04	0.01	0.75	0.09
25	$2.67*10^{16}$	5.56	0.93	0.09	0.03	0.79	0.16
50	$4.00*10^{32}$	5.23	0.94	0.17	0.04	0.81	0.25
100	$4.11*10^{12}$	2.29	0.89	0.27	0.59	0.71	0.45
150	$2.05*10^5$	0.98	0.77	1.03	0.13	0.50	1.51

Table 5.Thermodynamic parameters of Cu(II) adsorption on Clay and N-Clay

Adsorbent	Temperature °K	ΔS^o kJ·mol^{-1}·K^{-1}	ΔH^o kJ·mol^{-1}	ΔG^o kJ·mol^{-1}
Clay	298.15			-31.372
	308.15	0.039	20.002	-32.519
	318.15			-32.667
	328.15			-32.577
N- Clay	298.15			-33.203
	308.15	-0.029	42.192	-33.384
	318.15			-33.685
	328.15			-32.057

CONCLUSION

Investigation of Cu(II) removal from aqueous solution confirmed a higher capacity and a strong affinity by N-Clay particles derived from Egyptian alluvial clay soil compared to its clay fraction. Adsorption kinetics showed that more than 85% of Cu(II) ions were removed by N-Clay within the first 30 min which suggests two main mechanisms of adsorption, namely; ion exchange process at the interlayed permenant charge sites and inner-sphere complexes form on the hydroxyl edge sites. The pseudo-second order model was the best fit to adsorption kinetics. Data of adsorption isotherms was best fitted to Langmuir equation and the equilibrium contants indicated a favourable adsorption process of

Cu(II) on both the two adsorbents. The current study revealed that the Clay and N-Clay are considered efficient, low cost and eco-friendly adsorbents for Cu(II) removal from polluted aqueos environments. Future research is needed to investigate the performnce of these adsorbents in multi-heavy metals, cations, anions and organic ligands aqueous media similar to those found in local urban and industrial wastewater.

REFERENCES

Adebowale, K. O., E. I. Unuabonah, and B. I. Olu-Owolabi. 2008. Kinetic and thermodynamic aspects of the adsorption of Pb^{2+} and Cd^{2+} ions on tripolyphosphate-modified kaolinite clay. Chem. Eng. J., 136(2): 99-107.

Al-Anber, Z. A. and M. A. Al-Anber. 2008. Thermodynamics and kinetic studies of iron (III) adsorption by olive cake in a batch system. J. Mexican chem. Soc., 52(2): 108-115.

Angove, M. J., B. B. Johnson, and J. D. Wells. 1998. The influence of temperature on the adsorption of cadmium (II) and cobalt (II) on kaolinite. J. Colloid Interface Sci., 204(1): 93-103.

Argun, M. E. and S. Dursun. 2008. A new approach to modification of natural adsorbent for heavy metal adsorption. Bioresour. Technol., 99(7): 2516-2527.

Ayawei, N., A. N. Ebelegi, and D. Wankasi. 2017. Modelling and interpretation of adsorption isotherms. J. Chem., 57(4): 36-53.

Bergaya, F. and M. Vayer. 1997. CEC of clays: measurement by adsorption of a copper ethylenediamine complex. Appl. Clay Sci., 12(3): 275-280.

Bhattacharyya, K. G. and S. S. Gupta. 2006. Adsorption of Fe (III) from water by natural and acid activated clays: studies on equilibrium isotherm, kinetics and thermodynamics of interactions. Adsorpt., 12(3): 185-204.

Bhattacharyya, K. G. and S. S. Gupta. 2008. Influence of acid activation on adsorption of Ni (II) and Cu (II) on kaolinite and montmorillonite: kinetic and thermodynamic study. Chem. Engin. J., 136(1): 1-13.

Bhattacharyya, K. G. and S. S. Gupta. 2011. Removal of Cu (II) by natural and acid-activated clays: An insight of adsorption isotherm, kinetic and thermodynamics. Desalination, 272(1): 66-75.

Brown, G. 1984. Crystal structures of clay minerals and related phyllosilicates. Philosophical Transactions of the Royal Society of London. Series A, Mathemat. Phys. Sci., 311(1517): 221-240.

Chen, H., Y. Zhao and A. Wang. 2007. Removal of Cu(II) from aqueous solution by adsorption onto acid-activated palygorskite. J. Hazard. Mater., 149(2): 346-354.

Chotpantarat, S. and N. Kiatvarangkul. 2018. Facilitated transport of cadmium with montmorillonite KSF colloids under different pH conditions in water-saturated sand columns: Experiment and transport modelling. Water Res., 146: 216-231.

Christidis, G. and T. Marcopolous.1992. Kaolinite Generating Processes in the Milos Bentonites and Their Influence on the Physical Properties of Bentonites. The 6th International Congress of the Geological Society of Greece, Athens, 25-27 May 1992. 28-29.

Churchman, G. J., W. P. Gates, B. K. G. Theng and G. Yuan. 2006. Clays and clay minerals for pollution control. Dev. Clay Sci., 1(14): 625-675.

Cintrón Alvarado, I. A., T. Glotch and C. Che. 2008. X-RAY Characterization of Clay Minerals and Their Thermal Decomposition Products, American Geophysical Union, Fall Meeting.

Crini, G. and P. M. Badot (Eds.). 2010. Sorption processes and pollution: conventional and non-conventional sorbents for pollutant removal from wastewaters. Presses Univ. Franche-Comté.

Dal Bosco, S. M., R. S. Jimenez, C. Vignado, J. Fontana, B. Geraldo, F. C. A. Figueiredo and W. A. Carvalho. 2006 . Removal of Mn (II) and Cd (II) from wastewaters by natural and modified clays. Adsorption, 12(2): 133-146.

Eren, E. and B. Afsin.2008. An investigation of Cu (II) adsorption by raw and acid-activated bentonite: A combined potentiometric, thermodynamic, XRD, IR, DTA study. J. Hazard. Mater., 151(3): 682-691.

Flogeac, K., E. Guillon, M. Aplincourt, E. Marceau, L. Stievano, P. Beaunier and Y. M. Frapart. 2005. Characterization of soil particles by X-ray diffraction (XRD), X-ray photoelectron spectroscopy (XPS), electron paramagnetic resonance (EPR) and transmission electron microscopy (TEM). Agron. Sustain. Dev., 25(3): 345-353.

Gu, X., L.J. Evans and S.J. Barabash. 2010. Modeling the adsorption of Cd(II), Cu(II), Ni(II), Pb(II) and Zn(II) on to montmorillonite. Geochim. Cosmochim. Acta; 74: 5718–28.

Islam, M. A., M. M. Khan and M. S. Mozumder. 2004. Adsorption equilibrium and adsorption kinetics: a unified approach. Chem. Eng. Technol., 27(10): 1095-1098.

Jain, C. K. and M. K. Sharma.2002. Adsorption of cadmium on bed sediments of river Hindon: Adsorption models and kinetics. Water, Air, Soil Pollut., 137(1): 1-19.

Karabulut S., A. Karabakan, A. Denizli and Y. Yurum. 2000. Batch removal of copper(II) and zinc(II) from aqueous solutions with low-rank Turkish coals. Sep. Purif. Technol., 18: 177–184.

Kianfar, A. H., W. A. K. Mahmood, M. Dinari, M. H. Azarian and F. Z. Khafri. 2014. Novel nanohybrids of cobalt (III) Schiff base complexes and clay: Synthesis and structural determinations. Spectrochim. Acta Part A: Mol. Biomol. Spectrosc., 127: 422-428.

Kishk, F. M., H. A. El-Attar, M. N. Hassan and H. El-Sheemy. 1976. Mineralogical and chemical composition of the clay fraction of some Nile alluvial soils in Egypt. Chem. Geol., 17: 295-305.

Kuila, U. and M. Prasad. 2013. Specific surface area and pore-size distribution in clays and shales. Geophys. Prospect., 61(2): 341-362.

Kunze, G. W. and J. Dixon. 1986. Pretreatment for mineralogical analysis. Methods of Soil Analysis: Part 1 Physical and Mineralogical Methods., 5: 91-100.

Kurniawan, T. A. and W. H. Lo. 2009. Removal of refractory compounds from stabilized landfill leachate using an integrated H_2O_2 oxidation and granular activated carbon (GAC) adsorption treatment. Water Res., 43(16): 4079-4091.

Landry, V., B. Riedl, and P. Blanchet. 2008. Nanoclay dispersion effects on UV coatings curing. Prog. Org. Coat., 62(4): 400-408.

Le Roux, J. D., A. W. Bryson and B. D. Young. 1991. A comparison of several kinetic models for the adsorption of gold cyanide onto activated carbon. J.of the S. Afr. Inst. Min. Metall., 91(3): 95-103.

Madejová, J. 2003. FTIR techniques in clay mineral studies. Vib. Spectrosc., 31(1): 1-10.

Madejova, J. and P. Komadel. 2001. Baseline studies of the clay minerals society source clays: infrared methods. Clays Clay Miner., 49(5): 410-432.

Manohar, D. M., K. A. Krishnan, and T. S. Anirudhan. 2002. Removal of mercury (II) from aqueous solutions and chlor-alkali industry wastewater using 2-mercaptobenzimidazole-clay. Water Res., 36(6): 1609-1619.

Mockovčiaková, A. and Z. Orolínová. 2009. Adsorption properties of modified bentonite clay. Chem. Technol., 1(50): 47-50.

Mostafa, M. K. and R. W. Peters. 2016. Improve effluent water quality at Abu-Rawash wastewater treatment plant with the application of coagulants. Water Environ. J., 30(2): 88-95.

Mukasa-Tebandeke, I. Z., P. J. M. Ssebuwufu, S. A. Nyanzi, A. Schumann, G. W. A. Nyakairu, M. Ntale and F. Lugolobi. 2015. The elemental, mineralogical, IR, DTA and XRD analyses characterized clays and clay minerals of Central and Eastern Uganda. Adv. Mater. Phys. Chem., 5: 67-86

Murley L. 1992. Pollution Handbook. Brighton, National Society for Clean Air and Environmental Protection. Brighton, UK.

Oei, B. C., S. Ibrahim, S. Wang and H. M. Ang. 2009. Surfactant modified barley straw for removal of acid and reactive dyes from aqueous solution. Bioresour. Technol., 100(18): 4292-4295.

Osabor, V. N., P. C. Okafor, K. A. Ibe and A. A. Ayi. 2009. Characterization of clays in Odukpani, south eastern Nigeria. African J. Pure Appl. Chem., 3(5): 079-085.

Ouhadi, V. R., M. Amiri and A. R. Goodarzi. 2012. The special potential of nano-clays for heavy metal contaminant retention in geo-environmental projects: 631-642

Page, A. L. and A. Klute. 1986. Methods of soil analysis. Part 1. Physical and mineralogical methods; Part 2. Chemical and microbiological properties. American Society of Agronomy, Inc.

Peter, B. 1986. Mineral Powder Diffraction File, Search manual, Data book, Joint Committee on Powder diffraction Standards data cards (JCPDS), JCPDS International Center for Diffraction Data: 2-45

Pimneva, L. 2017. Adsorption of copper ions of natural montmorillonite clay. In MATEC Web of Conferences. 106: 03008.

Rezvani, P. and M. M. Taghizadeh. 2018. On using clay and nanoclay ceramic granules in reducing lead, arsenic, nitrate, and turbidity from water. Appl. Water Sci., 8(5): 1-6.

Malamis, S. and E. Katsou. 2013. A review on zinc and nickel adsorption on natural and modified zeolite, bentonite and vermiculite: Examination of process parameters, kinetics and isotherms. J. Hazard. Mater. 252: 428–461.

Schlumberger, J. 1987. Log Interpretation Principles/Applications. Schlumberger Education Services, Houton: 69-94.

Sheela, T., Y. A. Nayaka, R. Viswanatha, S. Basavanna and T. G. Venkatesha. 2012. Kinetics and thermodynamics studies on the adsorption of Zn (II), Cd (II) and Hg (II) from aqueous solution using zinc oxide nanoparticles. Powder Technol., 217: 163-170.

Sipos, P., R. Balázs and T. Németh. 2018. Sorption properties of Cd, Cu, Pb and Zn in soils with smectitic clay mineralogy. Carpathian J. Earth Environ. Sci., 13(1): 175-186.

Sivasaravanan, S. and V. B. Raja.2014. Impact characterization of epoxy LY556/E-glass fibre/nano clay hybrid nano composite materials. Procedia Eng., 97: 968-974.

Soleimani, M. and Siahpoosh, Z. H. 2015. Ghezeljeh nanoclay as a new natural adsorbent for the removal of copper and mercury ions: Equilibrium, kinetics and thermodynamics studies. Chin. J. Chem. Eng.., 23(11): 1819-1833.

Soleimani, M. and Z. H. Siahpoosh. 2016. Determination of Cu (II) in water and food samples by Na^+-cloisite nanoclay as a new adsorbent: Equilibrium, kinetic and thermodynamic studies. J. Taiwan Inst. Chem. Eng., 59: 413-423.

Sondi, I., Milat, O. and V. Pravdić.1997. Electrokinetic potentials of clay surfaces modified by polymers. J. Colloid Interface Sci., 189(1): 66-73.

Sondi, I., M. Stubičar and V. Pravdić. 1997. Surface properties of ripidolite and beidellite clays modified by high-energy ball milling. Colloids Surf., A: Physicochem. Eng. Aspects, 127(3): 141-149.

Ucun, H., Y.K. Bayhan and Y. Kaya. 2008. Kinetic and thermodynamic studies of the biosorption of Cr(VI) by Pinus sylvestris Linn. J. Hazard. Mater., 153 (1): 52-59.

Uddin, M. K. 2017. A review on the adsorption of heavy metals by clay minerals, with special focus on the past decade. Chem. Eng. J., 308: 438-462.

Vdović, N., I. Jurina, S. D. Škapin and I. Sondi.2010. The surface properties of clay minerals modified by intensive dry milling-revisited. Appl. Clay Sci., 48(4): 575-580.

Vertuccio, L., G. Gorrasi, A. Sorrentino and V. Vittoria. 2009. Nano clay reinforced PCL/starch blends obtained by high energy ball milling. Carbohydr. Polym., 75(1): 172-179.

Volzone, C., P.E. Zalba and E. Pereira. 1988. Activación ácida de esmectitas. II- Estudo mineralogico. An. Asoc. Quím. Argent., 76: 57-68.

Wang, X. S., H. Q. Hu and C. Sun. 2007. Removal of copper (II) ions from aqueous solutions using Na-mordenite. Sep. Sci. Technol., 42(6): 1215-1230.

Weaver,R., Kissel, D. E. Chen, F. L. T. West, W. Adkins, D. Rickman and J. C. Luvall. 2005. Mapping soil pH buffering capacity of selected fields in the Coastal Plain. Soil Sci. Soc. Am. J. 68:662–668.

WHO. 1971: International Standards for Drinking Water. Geneva, WHO.

Yavuz, Ö., Y. Altunkaynak and F. Güzel. 2003. Removal of copper, nickel, cobalt, and manganese from aqueous solution by kaolinite. Water Res., 37(4): 948-952.

Yong, R. N., B. P. Warkentin, Y. Phadungchewit and R. Galvez. 1990. Buffer capacity and lead retention in some clay materials. Water, Air, Soil Pollut., 53(1): 53-67.

Yu, B., Y. Zhang, A. Shukla, S. S. Shukla and K. L. Dorris. 2001. The removal of heavy metals from aqueous solutions by sawdust adsorption - removal of lead and comparison of its adsorption with copper. J. Hazard. Mater., 84(1): 83-94.

الملخص العربي

فاعلية حبيبات الطين النانوية المشتقة من التربة الطميية المصرية في إزالة أيونات النحاس الثنائية من المحاليل المائية

إيمان ماهر صالح، فوزي محمد كشك، رمزي مرسى هدية ، أحمد عبد الله الشافعى ، منى محمود عبد اللطيف

تساهم الإزالة الفعالة لأيونات النحاس (Cu^{+2}) من المياه العادمة الملوثة بشكل كبير في معالجتها وإعادة استخدامها. كانت أهداف هذه الدراسة هي إعداد وتوصيف حبيبات طينية بحجم النانو من تربة رسوبية لدلتا النيل وفهم وتقييم فعاليتها في إزالة أيونات النحاس (Cu^{+2}) من المحاليل المائية. تم تحضير جزيئات الطين النانوية عن طريق الطحن الكروي للمكون الطيني من التربة. وتم تأكيد مقياس النانو من خلال التصوير بميكروسكوب المسح الإلكتروني (SEM). وأوضحت نتائج تحليل حيود الأشعة السينية (XRD) سيادة معادن المونتموريلونيت في طين التربة وحبيبات الطين النانوي. كما أشارت نتائج تحليل منحنيات امتصاص الأشعة تحت الحمراء (FTIR) إلى وجود المجموعات الوظيفية السطحية المميزة لطين السميكتيت لكل من سطحي الإدمصاص. وقد أوضحت نتائج التجارب زيادة الإدمصاص لأيونات النحاس على أسطح الطين وحبيباته النانوية مع زيادة

كل من: التركيز الأولي (من 10 إلى 150 مجم /لتر)، تركيز حبيبات مادة الإدمصاص (0.05 ، 0.1 ، 0.25، 0.5 ، 1 جم / 100 مل) والرقم الهيدروجيني (4 ، 7 ، 9). كما أظهرت أسطح الإدمصاص مقاومة عالية لتغير قيم الرقم الهيدروجيني. أبدت حبيبات الطين النانوي قدرة على إزالة كمية أكبر من أيونات النحاس (62٪) مقارنة بطين التربة (45٪) عند تركيز إبتدائي 50 جزء في المليون من أيونات النحاس. وتم الوصول إلى حالة الاتزان خلال 30 دقيقة والذي تم تحقيقه في ظل ظروف تجريبية مختلفة، والتي تشير إلى آلية التبادل الأيوني. ودلت التحليلات الإحصائية ملائمة نتائج منحنيات الإدمصاص عند درجات حرارة متساوية وحركية الإدمصاص ملائمة نموذج لانجموير(Langmuir) ومعادلة الدرجة الثانية (Pseudo-second order) لوصف هذه النتائج على التوالى.